Transmission Kikuchi diffraction from nano-crystalline Ti and TiN thin-films

T Mungole[1], **J Zhang**[1], **B Mansoor**[2], **G Ayoub**[2, 3], **D P Field**[1]

[1] School of Mechanical and Materials Engineering, Washington State University, Pullman, Washington, 99164-2920, USA, PO Box 642920

[2] Mechanical Engineering Program, Texas A & M University, Doha, Qatar, PO Box 23874.

[3] Industrial and Manufacturing Systems Engineering Department, University of Michigan, Dearborn, Michigan USA 48128-2406

E-mail: tarang.mungole@wsu.edu

Abstract. Nano-crystalline Ti and TiN thin-films fabricated on <100> P-type Si wafers via magnetron sputtering are characterized by transmission Kikuchi Diffraction (TKD) in an FEI Sirion scanning electron microscope (SEM). A simple and cost-effective sample preparation combined with the TKD experiment at working distance of ~ 3 mm and a tilt of 35º produced indexable Kikuchi patterns. Pole figures generated by automatic and manual indexing revealed <0001>|| normal direction (ND) fiber texture and <111>||ND fiber texture in monolithic Ti and TiN thin-films, respectively. Glancing angle x-ray diffraction results corroborated the texture in the samples. Spatial resolution of ~ 60 nm is achieved that is close to the limit of resolution in conventional electron backscatter diffraction (EBSD). It is demonstrated that a simple sample preparation method in TKD technique combined with selected area electron diffraction (SAED) in transmission electron microscope (TEM) may reveal fundamental knowledge about different mechanisms occurring during fabrication and processing of the thin-film systems.

The fact that electron diffraction techniques can be successfully utilized in the determination of crystal structure, lattice strain and the grain orientations is now well established and has matured quite significantly after its first experimental observation in 1927 [1]. These diffraction experiments are now routinely performed in scanning electron microscope (SEM) as electron backscattered diffraction (EBSD) (or with electron channeling pattern (ECP)) and transmission Kikuchi diffraction (TKD); or in transmission electron microscope (TEM) as selected area electron diffraction (SAED) and convergent beam electron diffraction (CBED). EBSD utilizes the backscattered electrons for generating backscattered Kikuchi pattern (BKP) whereas TKD uses transmission Kikuchi patterns in the SEM. The SAED technique uses a parallel electron beam whereas a more detailed analysis is performed using CBED that uses a conical electron beam allowing to reveal full 3D symmetry of a crystal. Although TEM offers a good tool for working in the high resolution regime (few nm or less), it has its limitations such as reduced specimen area observation, specimen thickness limits, poor cost-effectiveness and is preferred mostly for the study of crystal defects. While TKD in the SEM has some of these same limitations, TKD offers a greater field of view and thus provides larger specimen area observation, which often makes TKD a precursor before going further to TEM operations. Furthermore, the crystal orientation measured in TEM is less accurate than in EBSD, latter of which has a stable accuracy of ~ 0.5º [2]. Therefore, recently, there has been a tremendous effort to increase the spatial resolution achievable in SEM for EBSD and TKD techniques [3]. A resolution of 20 nm has been achieved in EBSD [4] whereas in the case of TKD, a much better resolution of ~ 2-5 nm has been reported [5, 6]. However, in general, a spatial resolution of ~20 nm is difficult to achieve with ease in most modern SEMs and EBSD systems. Additionally, the reported resolution values of ~ 2-5 nm in TKD are for the best-case scenario and not an expected practical range for TKD. Nonetheless, due to a specimen tilt angle of ~ 70º in EBSD, the resolution down the tilt direction is about three times lower than the lateral resolution. Therefore, success of EBSD in characterizing nano-crystalline (NC) and nanostructured materials becomes limited.

The fundamental difference between TKD and EBSD is that the former exploits the very small thickness (tens of nm) of the specimen and a tilt of ~20-40° away from the EBSD detector to transmit and emit the inelastically scattered electrons from the back of the specimen. Consequently, Kikuchi pattern is generated from a small diffraction volume that leads to an improved spatial resolution.

High resolution becomes important in the case of characterization of thin-films as they mostly consist of small grain sizes. Metal-ceramic multilayer (MCM) thin-film systems are well-known for their promising mechanical and chemical properties as a result of which they are used widely for extreme environment applications. Exceptional properties are usually achieved in MCMs at nano-scales having domain sizes (i.e. layer thickness or grain sizes) < 10 nm [7, 8]. These remarkable properties are much dependent on their crystal/interface structure. In perspective of the abovementioned limitations of the use of EBSD at NC sizes, we apply TKD technique to successfully analyse NC grain structure and crystallographic texture in thin-films consisting of a metal (Ti) and ceramic (TiN) that leads to a spatial resolution of ~ 60 nm.

Thin-films consisting of monolithic Ti and TiN as well as an MCM consisting of alternating layers of Ti and TiN were fabricated via physical vapour deposition (PVD) by magnetron sputtering on <100> P-type Si wafers. TiN was deposited non-reactively by radio-frequency (RF) sputtering using a TiN compound target (2 in. diameter, Goodfellow, 99.99 % purity) at 300 W and an Ar pressure of 1.7×10^{-3} Torr. Ti was deposited via direct current (DC) sputtering using a Ti target (2 in. diameter, Goodfellow, 99.99 % purity) at 100 W and an Ar pressure of 1.6×10^{-3} Torr. A high modulation ratio (η) (i.e. h_{TiN}/h_{Ti}) of ~ 17.5 was ensured for the MCM sample whereas thickness of both monolithic Ti and TiN films was ~ 90 nm. Thickness of individual Ti and TiN layers in the MCM was ~ 1.7 nm and 33 nm, respectively. A high modulation ratio between ceramic/metal was chosen because of the fact that it facilitates high strain hardening rate [7] leading to remarkable mechanical properties in MCMs, in general.

Structure of the samples were characterized via glancing-angle x-ray diffraction (GXRD) at an incidence angle of 3°, and by diffraction and imaging techniques in SEM and TEM, details of which will be mentioned in the following sections. TEM sample preparation involved scratching of the thin-films by a diamond scribe and placing the powders on carbon coated Formvar® TEM grids. Mechanical characterization is conducted to determine the hardness by Nanoindentation technique using a Berkovich tip as instructed by the Oliver-Pharr method [9]. Monolithic and the multilayer films were re-deposited in order to have the total thickness close to ~ 600 nm to minimize the effect of the substrate during Nanoindentation.

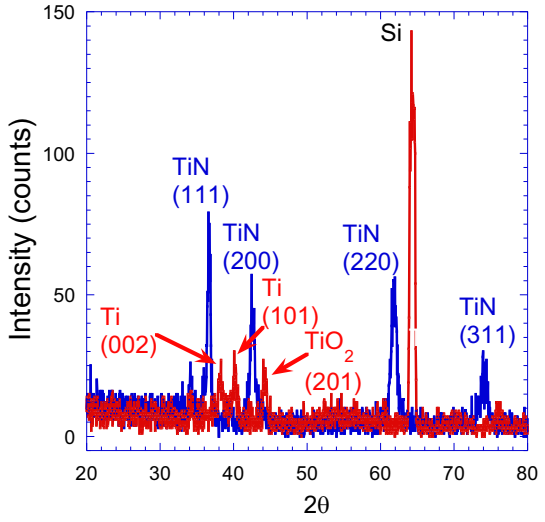

Figure 1. GXRD scan from monolithic TiN and Ti films deposited on <100> P-type Si. Crystalline nature of films is validated. Bragg reflections are clearly indexed showing a weak (111) orientation in TiN film.

Figure 1 shows the glancing angle x-ray diffraction (GXRD) 2θ-scans on monolithic Ti and TiN. Clearly indexed Ti (002), (101) and TiN (111), (200), (220) and (311) Bragg reflections are observed and it is realized that the films are crystalline. Rutile-TiO_2 phase is also detected which is due to high affinity of Ti towards oxygen. A weakly preferred (111) orientation in the monolithic TiN film is observed. Ti film shows

a weakly preferred (0001) orientation. Approximate crystallite size was roughly estimated by using Scherrer equation ($D = K\lambda/\beta\cos\theta$), where K is a dimensionless shape factor, λ is the x-ray wavelength, β is full width at half maximum intensity and θ is the Bragg angle. Estimated crystallite domain size is ~ 15 nm for TiN and ~ 40 nm for Ti. It is concluded from the x-ray diffraction experiments that the monolithic films consist of NC structure and follow growth by surface energy minimization.

Owing to the presence of small grain sizes in the thin-films, TKD was conducted on the monolithic Ti and TiN thin-films in an FEI Sirion SEM to evaluate the crystallographic texture and the microstructure. Recently, TKD has been successfully performed on numerous thin-films including that of Ni [10, 11], Al [12], Cu [13], Si [14] and oxide thin-films [15, 16, 17]. A spatial resolution of less than 10 nm has been achieved in several of these experiments. Common sample preparation technique for TKD consists of producing thin foils of the films using a focused ion-beam (FIB). However, in the current investigation, TKD experiments were performed on samples produced by breaking the Ti and TiN thin-films deposited on Si wafer followed by mounting the small wafer pieces on a sample holder consisting of a sweep cut 45° wedge (figure 2a) away from the EBSD detector with a silver paste. Thin-film side of the wafer always pointed away from the incident electron beam. Thorough search for locations with electron transparent sections near to the Si wafer edges consisting of protruding thin-films was conducted afterwards. Although this technique relies substantially on statistical distribution of the electron transparent sections over the edges, given a systematic routine of random observations, it is demonstrated in the current paper that this technique can provide reliable crystallographic data. Similar sample preparation techniques have been implemented in analysing nanoparticles [10, 16]. Due to the presence of 45° wedge on the sample holder, an SEM tilt of 10° was required to achieve a specimen tilt of ~ 35° as shown in figure 2b. A working distance of ~3 mm and beam accelerating voltage ranging from 20-30 kV, depending on the possible different sample thicknesses at different locations, allowed sufficient scattering to produce detectable transmission Kikuchi patterns.

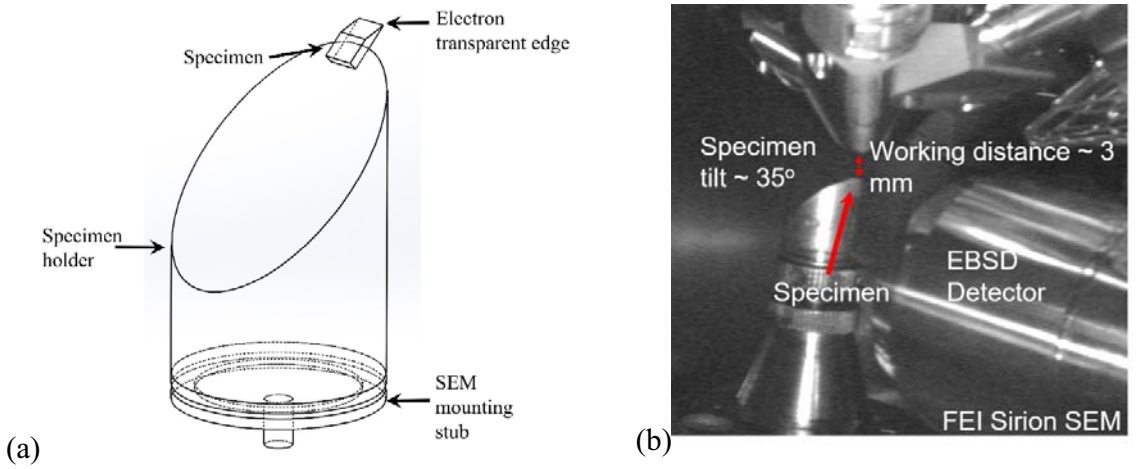

Figure 2. Setup to perform transmission Kikuchi diffraction in an FEI Sirion SEM. (a) broken thin-film sample mounted on a specimen holder and (b) tilted to 35° away from the detector at a working distance of ~ 3 mm. 45° wedge on the specimen holder allows 10° tilt in the SEM.

Figure 3 displays the SEM image of electron transparent sections from the monolithic Ti and TiN thin-films, respective TKD patterns and an image quality map from the Ti thin-film. figure 3a and figure 3b show the region of interest on Ti thin-film (circled) and the produced TKD pattern, respectively. It is realized that the Kikuchi pattern is clearly detectable with (0001) pole pointing towards the normal direction (ND) of the film. figure 3c displays the image quality (IQ) map from the region of interest. The TKD patterns were generally of poor quality in this sample. This is attributed to the sample preparation technique

due to which the sample surface normals, where the scattered electrons exit the backside of the sample, don't point coherently towards the detector. Thus, the orientation maps reconstructed from the TKD measurements are of insufficient quality to provide a representative estimate of the microstructure or texture. Nevertheless, the spatial resolution in Ti film can be successfully assessed from the IQ map. IQ map represents the sharpness/detectability of Kikuchi patterns, which is representative of crystalline defects in the sample. Although IQ differences from grain orientations are usually smaller than those due to the presence of grain boundaries, lattice strains and different phases, it is generally understood that grain boundaries produce diffused scattering and hence a low IQ. Therefore, from figure 3c, it can be deduced that relatively brighter regions are separated by dark regions signifying that they may be separated by grain boundaries. It can be noticed that the lateral grain size of ~ 60 nm is detected in Ti thin-film, which is not very different from the value (~ 40 nm) obtained from estimation of crystallite size from x-ray diffraction described earlier.

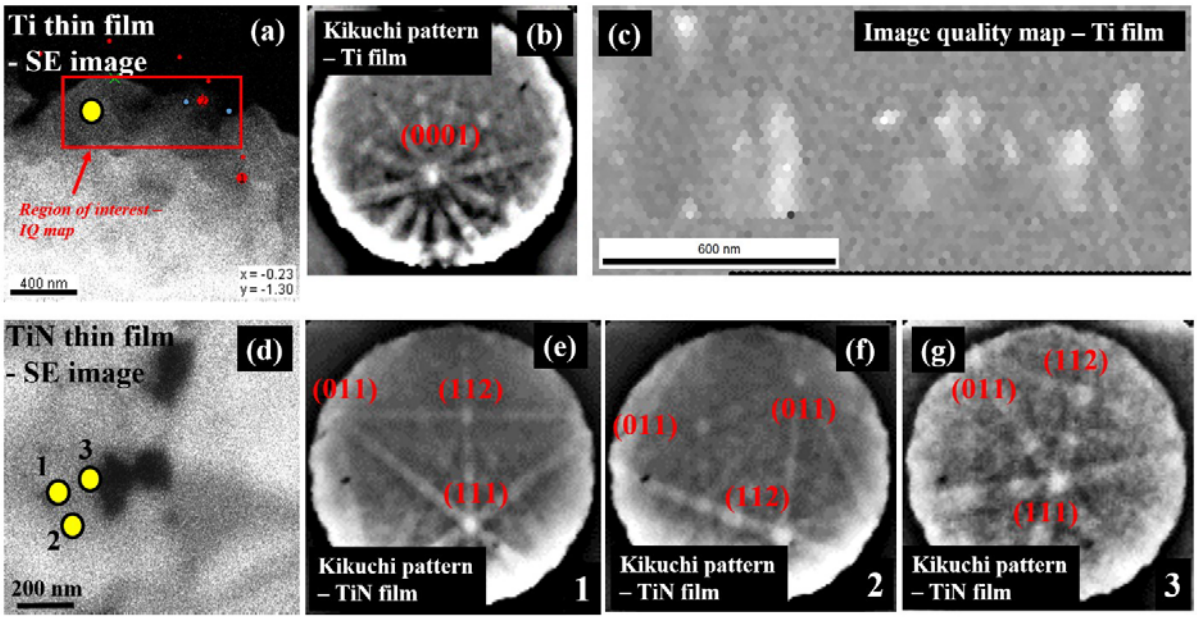

Figure 3. Results from transmission Kikuchi diffraction (TKD) on monolithic Ti and TiN thin-films showing region of electron transparent section in (a) Ti and (d) TiN, produced TKD patterns from (b) Ti and (e,f,g) TiN and (c) image quality map from the Ti thin-film. Region 1 and 2 produced faint TKD patterns (e,f) while from a thinner section at region 3 produced brighter TKD pattern (g). Spatial resolution of ~60 nm in Ti and ~80 nm in TiN thin-film can be estimated.

Figure 3d shows similarly an SEM image from the electron transparent region from the TiN thin-film. figure 3e and 3f show the indexed TKD patterns that are obtained from region 1 and 2 shown in figure 3d, respectively. These regions are relatively thicker as they are far from the edge of the electron transparent region of the TiN thin-film. It is noticed that the TKD patterns are less sharp and smeared out compared to that obtained in figure 3b. Region 3 is closer to edge which results in diffraction from a thinner section of the sample producing a sharper TKD pattern as shown in figure 3g. A lateral resolution of ~ 80 nm is obtained from the TiN thin-film. Additionally, detectable patterns were produced only from a limited region as shown in figure 3a and 3d and not from relatively thicker sections of the sample due to a higher as-deposited film thicknesses of ~ 90 nm for both Ti and TiN films. Furthermore, as the sample preparation technique involved breaking of coated Si wafers, thus facilitating an irregular path of crack propagation, that resulted in a majority of sample surface NDs facing away from the EBSD detector. These limitations combined with smeared TKD patterns inhibits automatic indexing of the patterns. This limits the diffraction

data obtained from the TKD experiment and prevents a precise calculation of spatial mapping of the orientations. Relatively low spatial resolution (~ 60 nm for Ti film and ~ 80 nm for TiN film) obtained in the current study is a result of such an artefact. The resolution values have been calculated respectively via the smallest grain in the IQ map and the average distance between points 1, 2 and 3 in figure 3d. These points are separated by the least distance where Kikuchi patterns start to deviate significantly from each other. Nevertheless it can be concluded that in the case of thin-films, a relatively simple sample preparation process combined with TKD experiments can be used to estimate microstructural information from NC grains in a thin-film system. Operation of conventional EBSD in these samples failed to produce any indexable Kikuchi patterns, thus implying an important role of TKD in the characterization of the thin-films.

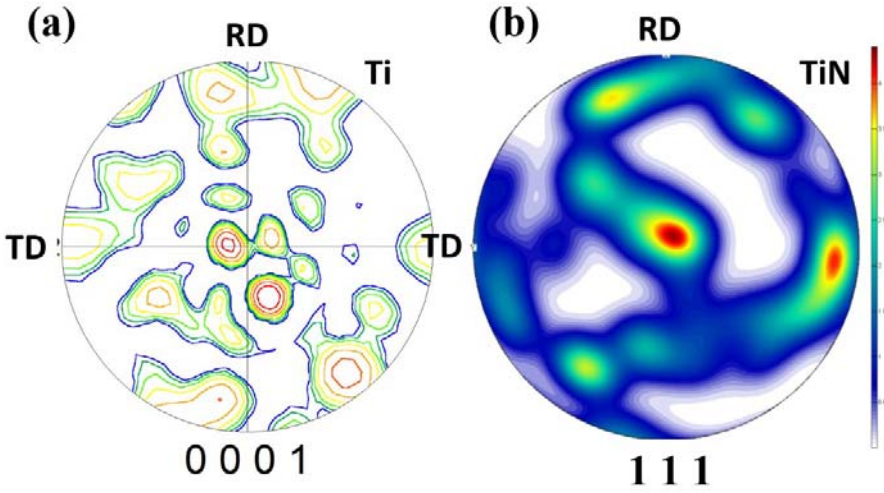

	φ_1	Φ	φ_2
1	38	48	27
2	34	51	216
3	24	113	189
4	17	19	0
5	17	19	0
6	309	74	51
7	285	108	45
8	329	84	72
9	120	125	144
10	120	125	144
11	120	125	144
12	120	125	144
13	195	125	144
14	216	132	168

Figure 4. Pole figures generated from automatic pattern indexing from (a) monolithic Ti and (b) from manual indexing from monolithic TiN thin-films via transmission Kikuchi diffraction (TKD). Approximate <0001>||ND and <111>||ND fiber texture are observed in Ti and TiN, respectively. (c) shows the raw Euler angles obtained from manual indexing in TiN thin-film to create the pole figure in (b).

Figure 4 shows pole figures obtained from analysis of the TKD patterns generated from monolithic Ti and TiN thin-films. Analyses were done using TSL OIM© v 7 and MTEX (in MATLAB©) software packages. As mentioned earlier, only a limited region on the sample produced detectable TKD patterns out of which only a few were automatically indexable. Therefore, a statistically significant data for pole figure calculation is contingent on the amount of data collected which is restricted by the relatively rigorous procedure of manual indexing. Nevertheless, as shown in figure 4a, automatic indexing of the TKD patterns produced crystallographic texture data representing a <0001>||ND fiber texture in monolithic Ti thin-film. This is in coherence with a weak basal texture obtained from x-ray diffraction data in figure 1. Pole figure for the monolithic TiN thin-film shown in figure 4b was generated after manually indexing of the TKD patterns. Crystallographic texture representing a <111>||ND fiber texture is observed. This is also in coherence with the x-ray diffraction data representing a weak (111) texture in TiN film. Figure 4c shows the Euler angles obtained after manual indexing of the patterns from TiN film, used to create pole figure in figure 4b. It should be noted that as the number of TKD patterns are not statistically significant, the pole figure data is not representative of the true crystallographic texture of the thin-films. This insufficiency is observed in approximate fiber texture represented in figure 4a and 4b. Nonetheless, texture calculations from the aforementioned procedure of sample preparation combined with TKD also enables an estimation of true crystallographic texture in thin-film system consisting of NC grains and nanostructures.

Figure 5 represents results from TEM and Nanoindentation analysis on the samples. It is clear from the cross-sectional bright field TEM image (figure 5a) of the multilayer sample that the microstructure consists of NC grains in TiN layer with approximate grain size of ~ 5-10 nm. The grain size is however very different than that obtained from the TKD analysis of monolithic TiN film. This can either be attributed to the effect of multilayering of the Ti and TiN layers inhibiting grain growth during the deposition process or to a relatively low resolution (~ 80 nm) obtained in the TKD analysis of the TiN sample as a consequence of limitations due to the sample preparation technique. The inset in figure 5a shows the selected area diffraction pattern (SADP) obtained from diffracting a significant volume of the multilayer sample in TEM. Clearly indexed diffraction rings as (111), (200), (220) and (311) pertaining to TiN layer are distinguished.

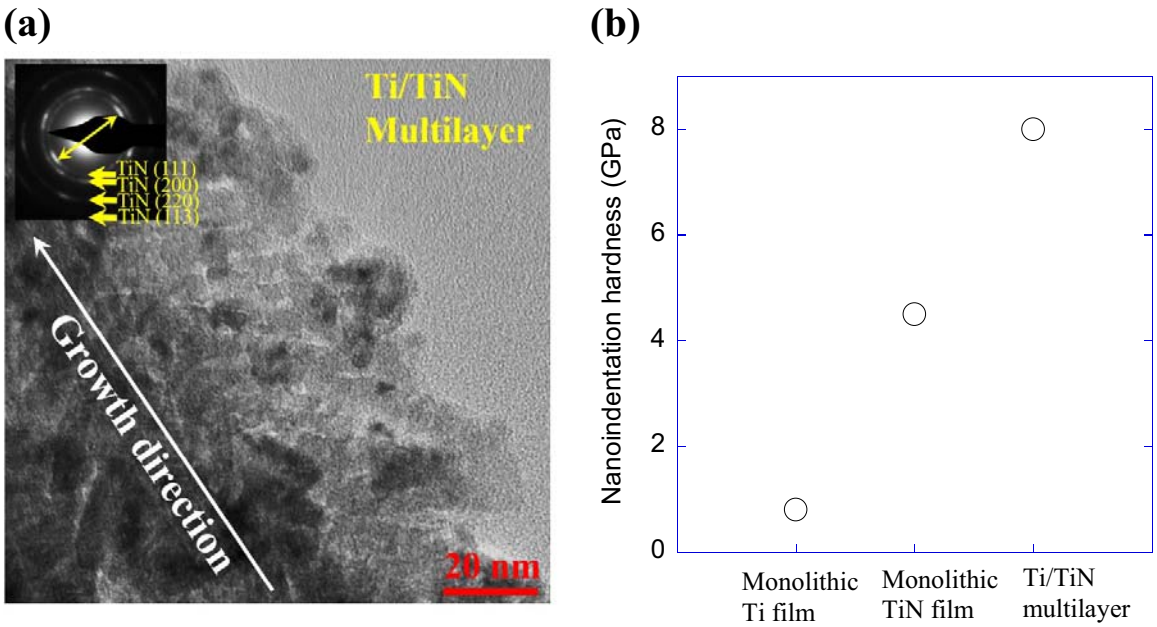

Figure 5. Characterization of the thin-film samples via (a) TEM showing in the inset the SADP image and (b) Nanoindentation showing hardness of the samples. It is realized that TiN layers in the multilayer sample has crystallite size ~ 5 nm with an in-plane orientation of (111) crystallographic planes leading to expected texture softening. Growth occurs by interface energy minimization in the multilayer sample. Multilayer hardness shows opposite trend depicting interface strengthening mechanisms.

It is however noted that the TiN layer does no longer show a fiber texture. Instead, (111) planes lie parallel to the ND of the film indicating an in-plane orientation of the closest packed planes. This transition of texture in TiN layer depicts a possible transition of growth mechanism during deposition from surface energy minimization in monolithic thin-films and a interface energy minization during multilayering of the two films. Also, the orientation of (111) planes lying parallel to the ND in TiN layer would predict texture softening in the multilayer sample as opposed to a hard orientation in the monolithic TiN thin-film pertaining to a low Schmid factor (i.e. <111>||ND) in the case compressive loading. figure 5b shows the Nanoindentation hardness of the samples. It is readily observed that the hardness of the samples increases significantly in the multilayer sample compared to its monolithic counterparts. However, the softening effect due by crystallographic texture predicts a lower hardness for the multilayer sample than predicted by the rule-of-mixtures. This indicates that there are other strengthening mechanisms such as interface acting as barriers to dislocations transmission during the deformation of the multilayer than in the monolithic Ti and TiN samples. It has been shown that interfaces act as significant obstacles to dislocation propagation for nano-scale multilayered structures, owing to the application of classical Hall-Petch relation extended to the realm of multilayered structures [8, 18].

In summary, it is shown that thin-films consisting of NC grains and nanostructures can be characterized to obtain approximate information about the microstructure and crystallographic texture via a simple and cost-effective sample preparation technique combined with TKD technique in an SEM. In spite of several shortcomings of this procedure, a spatial resolution of ~ 60 nm is achieved, making TKD an essential tool for investigating detailed crystallography of NC thin-films. Moreover, combination of TKD technique with other diffraction routines such a SAED in TEM in conjunction with mechanical characterization may reveal fundamental knowledge about different mechanisms occuring during fabrication and processing of the thin-film systems.

Acknowledgements

The authors acknowledge the support provided by Qatar National Research Fund (QNRF) under NPRP grant # 7-1470-2-528 for this work. QNRF is a constituent member of the Qatar Foundation.

References

[1] Thomson G P and Reid A 1927 *Nature* **119** 890
[2] Humphreys F J 2001 *J. Mater. Sci.* **36** 3833–54
[3] Suzuki S 2013 *JOM* **65** 1254–63
[4] Troost K and Kamminga J –D 1994 *Proc. Microscopy and Microanalysis*, *The Microscopy Society of America, USA* 606
[5] Trimby P W 2012 *Ultramicroscopy* **120** 16–24
[6] Brodusch N, Demers H and Gauvin R 2013 *J. Microsc.* **250** 1–14
[7] Wang J and Misra A 2014 *Curr. Opin. Sol. St. Mater. Sci.* **18** 19–28
[8] Misra A, Hirth J P and Hoagland R G 2005 *Acta Mater.* **53** 4817–24
[9] Oliver W C and Pharr G M 2011 *J. Mater. Res.* **7** 1564–83
[10] Keller R R and Geiss R H 2012 *J. Microsc.* **245** 245–51
[11] Kacher J, Hattar K and Robertson I M 2016 *Mater. Sci. Eng. A* **675** 110–9
[12] Zhang S Y, Zhang Y J, Kwek W M, Goi L S, Trigg A D and Tang L J 2014 *Proceedings of the 16th Electronics Packaging Technology Conference, EPTC*
[13] Lee S Y, Guim H U, Kim D I, Joo Y C, Shim C H, Ahn J P, Choi I S and Abbasi M 2017 *Scr. Mater.* **138** 52–6
[14] Fundenberger J J, Bouzy E, Goran D, Guyon J, Yuan H and Morawiec A 2016 *Ultramicroscopy* **161** 17–22
[15] Mortazavi N, Esmaily M and Halvarsson M 2015 *Mater. Lett.* **147** 42–5
[16] Geiss R H, Rice K P and Keller R R 2013 *Microsc. Microanal.* **19** 696–7
[17] Garner A, Gholinia A, Frankel P, Gass M, MacLaren I and Preuss M 2014 *Acta Mater.* **80** 159–171
[18] Misra A, Verdier M, Lu Y C, Kung H, Mitchell T E, Nastasi M and Embury J D 1998 *Scr. Mater.* **39** 555–60